ISSN 0023-1584, Kinetics and Catalysis, 2006, Vol. 47, No. 5, pp. 719–727. © MAIK "Nauka/Interperiodica" (Russia), 2006.
Original Russian Text © S.I. Pomogailo, V.G. Dorokhov, A.M. Lyakhovich, S.S. Mikhailova, G.I. Dzhardimalieva, A.D. Pomogailo, 2006, published in Kinetika i Kataliz, 2006, Vol. 47, No. 5, pp. 742–750.

Synthesis, Structure, and Catalytic Properties of Polymer-Immobilized Rhodium Clusters[1]

S. I. Pomogailo[a], V. G. Dorokhov[a], A. M. Lyakhovich[b], S. S. Mikhailova[b], G. I. Dzhardimalieva[a], and A. D. Pomogailo[a]

[a] *Institute of Problems of Chemical Physics, Russian Academy of Sciences, Chernogolovka, Moscow oblast, 142432 Russia*
e-mail: adpomog@icp.ac.ru

[b] *Physicotechnical Institute, Ural Division, Russian Academy of Sciences, Izhevsk, 426000 Russia*

Received April 13, 2005

Abstract—Immobilized Rh_6 clusters (cyclohexene hydrogenation catalysts) were prepared by the polymer-analogous transformations or copolymerization of cluster-containing monomers and characterized. Intermediates formed in the course of a catalytic reaction were studied using IR spectroscopy, XPS, and atomic force microscopy. It was found that the relative intensity of a low-energy line in the Rh3$d_{5/2}$ spectrum of the initial polymer-immobilized cluster in the XPS spectrum of Rh_6 increased in the course of hydrogenation. The catalytic activity of the immobilized complex changed symbatically with both the number of Rh atoms bound to the H(CO) group and the number of Rh atoms, the charge on which was greater than that in the parent cluster. Some experimental evidence was obtained in favor of the hypothesis of cluster fragmentation in the course of hydrogenation with the formation of highly active, most likely, nanosized particles, which are true catalysts, in low concentrations. The surface of macrocomplex particles after hydrogenation became more homogeneous and hydrophilic; this fact is also indicative of an increase in the concentration of polar functional groups in surface layers. This was likely due to Rh–Rh bond cleavage in the polymer-immobilized cluster.

DOI: 10.1134/S0023158406050107

INTRODUCTION

The immobilization of noble metal clusters on polymer supports is of interest as a technique for the development of efficient and selective catalysts. Size effects on catalytic activity can be monitored using these complexes as examples [1, 2]. It is of crucial importance to find out whether the cluster group remains unchanged in the course of catalytic reaction or undergoes transformations related to aggregation or segregation, whether the resulting metal centers remain structurally homogeneous, and how the molecular organization of immobilized complexes changes in this case. Answers to some of the above questions can be obtained by studying the binding of metal clusters to polymer supports because this procedure provides an opportunity to isolate and analyze intermediates formed in the course of catalytic reaction [3]. The aim of this work was to prepare the rhodium-containing polymer-immobilized clusters Rh_6 and to study their catalytic properties in the reaction of cyclohexene hydrogenation and concomitant transformations.

EXPERIMENTAL

$RhCl_3 \cdot 4H_2O$ (rhodium content 34.55%) and reagent-grade CO were used without additional purification. Solvents were purified and dried in accordance with standard procedures. The synthesis of $Rh_6(CO)_{16}$ (**1**) and $Rh_6(CO)_{15}CH_3CN$ (**2**) was performed in accordance with a published procedure [4].

The cluster-containing monomer $Rh_6(CO)_{14}(\mu,\eta^2\text{-}PPh_2CH_2CH{=}CH_2)$ (**3**) was prepared by the reaction of $Rh_6(CO)_{15}CH_3CN$ with diphenyl phosphoallyl (DPPA) in accordance with a procedure similar to that for the preparation of Os_3 clusters with DPPA [5]. Found (%): C, 27.51; H, 1.48; P, 2.47; Rh, 48.6. For $C_{29}H_{15}PRh_6O_{14}$ anal. calcd. (%): C, 28.18; H, 1.22; P, 2.51; Rh, 49.96. IR (ν, cm^{-1}; $CHCl_3$): 2092 m, 2055 s, 2040, 2018 (t-CO), 1790 (μ-CO), 1622 m (C=C), 1436 w, 1001 w (P–C).

Radical copolymerization was performed in bulk or in toluene. The weighed portions of an azobisisobutyronitrile (AIBN) initiator (0.6 mol %), cluster monomer **3**, and the solvent were placed in an ampule, and the contents were outgassed three times at a reduced pressure. Next, the ampule was sealed and transferred to a thermostat at 70°C. After a specified time, the ampule was opened and the target product was isolated by reprecipitation in methanol from a benzene solution, which was presaturated with argon, and dried in a vacuum to constant weight.

The synthesis of immobilized clusters by polymer-analogous transformations was performed in the following manner: Styrene and DPPA copolymers were

[1] Synthesis and Reactivity of Metal-Containing Monomers series, report 63.

Table 1. Characteristics of styrene and DPPA copolymers and immobilized $Rh_6(CO)_{15}CH_3CN$ clusters

DPPA (M_1) and styrene (M_2) copolymers				Macrocomplexes				
$M_1 : M_2$ (mol)	$\overline{M}_n$	$\overline{M}_w$	$\overline{M}_w/\overline{M}_n$	Rh-SDPPAC	[Rh], wt %	$\overline{M}_n$	$\overline{M}_w$	$\overline{M}_w/\overline{M}_n$
1 : 1	9600	26200	2.70	1-SDPPAC	1.87	9300	36100	3.88
1 : 3	20700	52900	2.55	2-SDPPAC	3.00	22300	90500	4.06
1 : 7.5	25600	95600	3.73	3-SDPPAC	3.18	60200	204200	3.39
1 : 40	80000	169000	2.11	4-SDPPAC	4.16	56000	140000	2.50

prepared by radical polymerization in the presence of AIBN (0.5 wt %) at 58°C for 3–6 h. The isolated copolymer was dissolved in benzene (0.2 g in 20 ml), and 0.02 g of the cluster $Rh_6(CO)_{15}CH_3CN$ in 5 ml of benzene was added with continuous magnetic stirring. After 30 min, the target product (a macromolecular complex) was precipitated with methanol, filtered off, and dried in a vacuum.

The molecular-weight characteristics of copolymers and macrocomplexes (number-average and weight-average molecular weights $\overline{M}_n$ and $\overline{M}_w$, respectively) were determined by gel permeation chromatography (Waters 200). The eluent was tetrahydrofuran.

For a comparative evaluation of the catalytic properties of polymer-immobilized catalysts, a 1% Rh/C typical low-percentage heterogeneous catalyst was prepared using an impregnation method [6]. For this purpose, 50 mg of $RhCl_3 \cdot 4H_2O$ was adsorbed from an aqueous solution onto 1.32 g of preactivated soot (S_{sp} = 850 m^2/g); thereafter, the sample was reduced with an excess of $NaBH_4$, and the product was dried at 100°C.

The catalytic hydrogenation of cyclohexene was performed in a thermostated reactor of the long-necked flask type with stirring. From 0.01 to 0.1 g of a catalyst was placed in the reactor so that the Rh amount in the portion was 3.9×10^{-5} g-at. The system was purged with hydrogen, and 15 ml of degassed isopropanol was added; the contents were stirred. After the completion of activation (15 min), 4.5 or 6.5 mmol of cyclohexene was added to the reactor. A solvent portion of 5 ml was used for washing. The reaction was performed at 40°C with intense stirring (300–400 swings per minute). The rate of reaction was evaluated from hydrogen consumption with time. Variation in replicate experiments was no higher than 5%.

IR spectra were recorded on a Specord M-80 spectrophotometer or a Perkin-Elmer 325 instrument in chloroform and KBr pellets, respectively.

An ES-2401 spectrometer with a magnesium anode was used for obtaining the XPS spectra. The X-ray tube power was 200 W; the residual pressure in the analyzer chamber was 10^{-6} Pa. The spectrometer was calibrated against the Au4$f_{7/2}$ line at 84 eV. The binding energy (E_b) of the line of C1*s* electrons in an alkyl group of saturated hydrocarbons was taken equal to 285.0 eV. The accuracy in the determination of line positions on the scale of binding energies was 0.1–0.2 eV; the mathematical processing of the spectra was performed in accordance with a published procedure [7]. $RhCl_3 \cdot 4H_2O$ was used as the reference sample in XPS analysis.

Atomic force microscopic studies were performed on a P-47 Solver instrument (NT-MTD) in accordance with a published procedure [8]. Silicon cantilevers from the same manufacturer were used; the needle curvature radius was ~10 nm. Test samples were prepared as a suspension in toluene, which was subsequently supported onto a glass-ceramic substrate and dried. Along with a topographic study, interacting forces (F_z, nN) between the microscope probe and the sample were determined. For this purpose, so-called cantilever deflection was measured as a function of the distance z between the probe and the sample (force–distance curves).

RESULTS AND DISCUSSION

Polymer-analogous transformations. Although attempts at chemically binding clusters to polymers have been made since the 1970s [9, 10], many important problems remain unsolved. First, this is true of a scientifically justified search for macroligands, reaction conditions, and the composition and characterization of the resulting products. Phosphorylated styrene and divinylbenzene copolymers or ternary styrene–divinylbenzene–vinyl(styryl)diphenylphosphine block copolymers are most frequently used as macroligands. It is well known that phosphorus-containing rhodium complexes (including polymeric complexes) are active and selective catalysts for reduction, hydroformylation, and other reactions [11, 12]. We used a copolymer of DPPA with styrene, which was prepared by free-radical copolymerization in the presence of an AIBN initiator.

The macrocomplexes were prepared by the interaction of $Rh_6(CO)_{15}CH_3CN$ with the synthesized macroligand (styrene and DPPA copolymers (SDPPACs)) in benzene at various ratios between monomers (M_1/M_2). In turn, the parent cluster complex $Rh_6(CO)_{15}CH_3CN$ with a labile acetonitrile ligand was prepared by the photolysis (UV radiation; $\lambda > 300$ nm) of $Rh_6(CO)_{16}$ in the presence of acetonitrile. Table 1 summarizes the main characteristics of the parent copolymers and macrocomplexes.

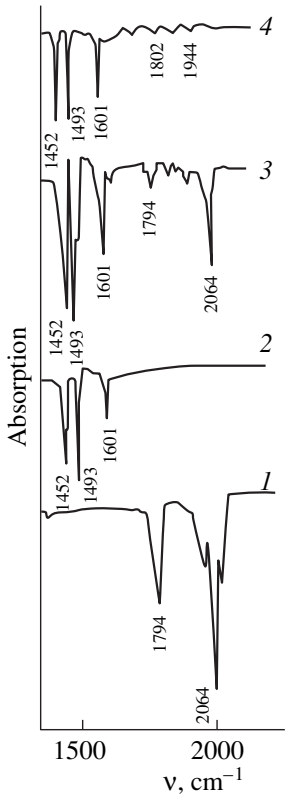

Fig. 1. IR spectra of (*1*) $Rh_6(CO)_{15}CH_3CN$, (*2*) DPPA and styrene copolymer, (*3*) $Rh_6(CO)_{15}CH_3CN$ immobilized on the DPPA and styrene copolymer (4-SDPPAC) before reaction, and (*4*) $Rh_6(CO)_{15}CH_3CN$ immobilized on the DPPA and styrene copolymer (4-SDPPAC) after cyclohexene hydrogenation.

IR-spectroscopic data (Fig. 1) indicate that the cluster structure of the metal grouping remains unaffected upon binding to a polymer: bands due to the stretching vibrations of terminal and bridging CO groups, which are characteristic of monosubstituted derivatives of $Rh_6(CO)_{16}$, were observed (2064–2066 and 1794–1802 cm^{-1}, respectively). The disappearance of the absorption band at 2294 cm^{-1}, which corresponds to the stretching vibrations of the CN group of coordinated acetonitrile in $Rh_6(CO)_{15}CH_3CN$, suggests substitution for the labile acetonitrile ligand. A similar behavior was observed in the interaction between a styrene and 4-vinylpyridine copolymer and $Rh_6(CO)_{15}CH_3CN$ [13] or $Os_3(CO)_{12}$ [14].

According to XPS data, as compared with the spectrum of $Rh3d_{5/2}$ electrons in $Rh_6(CO)_{16}$ (Fig. 2, spectrum *2*), additional low-energy lines with E_b = 308.2 and 307.1 eV appeared in the analogous spectra of the intermediate cluster complex $Rh_6(CO)_{15}CH_3CN$ and the macrocomplex on its basis (4-SDPPAC), respectively (Fig. 2, spectra *3*, *4*). This suggests a decrease in the positive charge on the Rh atom in the complexes [15, 16]. The presence of a line at E_b = 308.9 in the $Rh3d_{5/2}$ spectra of $Rh_6(CO)_{16}$ and the intermediate clus-

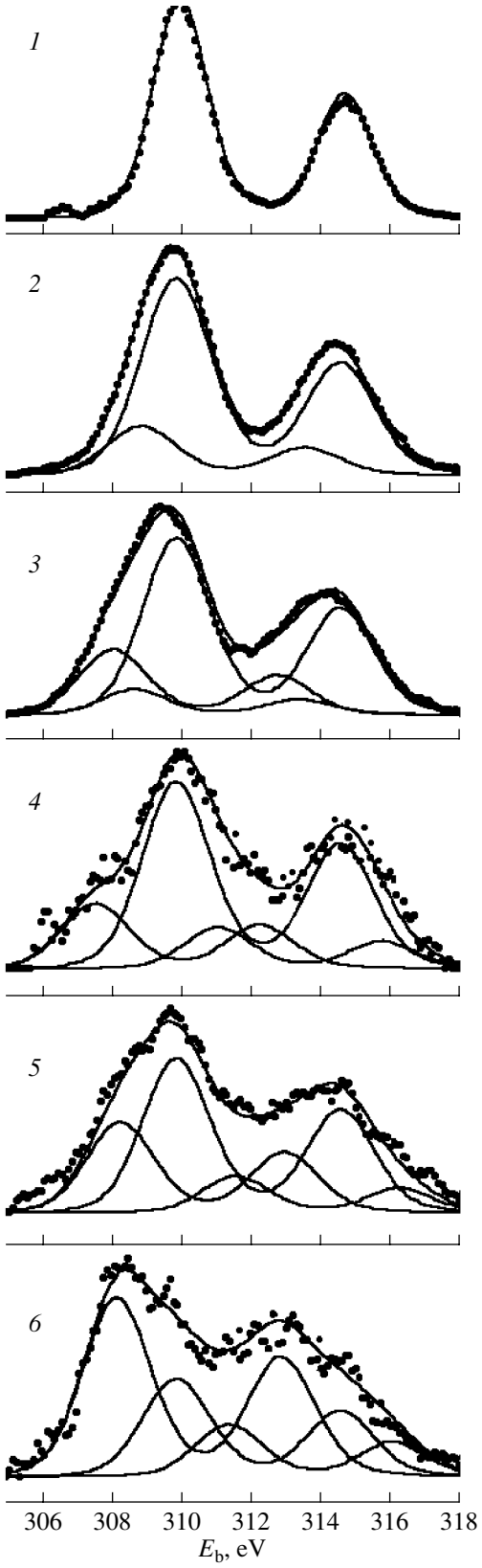

Fig. 2. Rh3*d* XPS spectra of (*1*) $RhCl_3 \cdot 4H_2O$, (*2*) $Rh_6(CO)_{16}$, (*3*) $Rh_6(CO)_{15}CH_3CN$, (*4*) 4-SDPPAC macromolecular cluster, and (*5*, *6*) the above cluster after the (*5*) first and (*6*) second hydrogenation cycles.

Table 2. Bulk copolymerization of the cluster monomer $Rh_6(CO)_{14}[\mu,\eta^2\text{-}PPh_2CH_2\text{–}CH{=}CH_2]$ (**3**) with styrene (70°C; 0.6 mol % AIBN)

Copolymer	Concentration of **1** in the monomer mixture, mol %	Concentration of cluster units in the copolymer, mol %	Concentration of Rh in the copolymer, wt %	$\overline{M}_n$
1	0.04	0.02	0.09	56600
2	0.08	0.1	0.6	33000
3	1.0	1.0	0.5	**
4*	1.0	1.4	1.4	**

*Copolymerization in toluene.

**Molecular weights were not determined.

ter complex $Rh_6(CO)_{15}CH_3CN$ is most likely a consequence of the decarbonylation of the clusters in a vacuum under the action of X-rays. A similar shift (0.9 eV) to lower binding energies was observed upon the loss of a CO group in $Rh(CO)_2$ [17]. Note that the $Rh3d_{5/2}$ spectrum of the parent compound $RhCl_3 \cdot 4H_2O$, which was used in the synthesis of the carbonyl cluster, contained a single line at $E_b = 310.0$ eV (Fig. 2, spectrum *1*), which is consistent with published data [18–20]. It is of interest that the reactions of metal cluster binding to a macroligand were not accompanied by deep processes of polymer degradation or crosslinking, although the molecular-weight distribution (M_n/M_w) of the metal polymers was somewhat broadened (Table 1).

Copolymerization of $Rh_6(CO)_{14}[\mu,\eta^2\text{-}PPh_2CH_2\text{–}CH{=}CH_2]$ (3) with styrene. Polymer-analogous transformation methods frequently provide an opportunity to obtain an expected result. However, they include many stages: the synthesis of a macroligand and a metal cluster, the reaction between them, and the removal of chemically unbound components. On the one hand, this considerably complicates the preparation process and decreases the yield of the desired product; on the other hand, this can be accompanied by a number of transformations in immobilized reactants. A single-step procedure for the preparation of polymer-bound clusters is largely free of the above disadvantages. In this procedure, the polymerization and copolymerization of cluster-containing monomers—cluster complexes whose ligand environment includes at least one group with multiple (most frequently, double) bonds, which are capable of polymerization reactions—are used. Previously [21], we prepared and characterized the cluster-containing monomer $[Rh_6(CO)_{14}(\mu,\eta^2\text{-}PPh_2CH_2CH{=}CH_2)]$ (**3**) with DPPA as an unsaturated ligand. This ligand was chosen because, as well as all of the allyl-type monomers, it is less reactive than vinyl derivatives in polymerization reactions because of degradation chain propagation. This allowed us to obtain copolymers with low rhodium contents—low-percentage rhodium catalysts.

The copolymerization of styrene with cluster monomer **3** was performed in the bulk. Because of the limited solubility of **3** in styrene, the maximum concentration of **3** in the monomer mixture was 1 mol %. As can be seen in Table 2, the molecular weights of the resulting copolymers decreased with the cluster comonomer content of the reaction mixture. This was likely due to the cluster nature of the comonomer, which is responsible for the specificity of the reactions that restrict chain growth. Note that, on going from the bulk copolymerization of **3** with styrene to the copolymerization in solution, the polymer yield decreased, but the concentration of cluster units in the copolymer increased (from 0.4 to 1.4 wt % Rh).

The presence of absorption bands that correspond to the stretching vibrations of bridging (1794 and 1802 cm^{-1}) and terminal CO groups (1942, 2017, 2064, and 2104 cm^{-1}) in the IR spectra suggests that the cluster monomer did not undergo considerable changes upon its insertion into a polymer molecule. This was also supported by XPS data. The binding energies (308.2 and 309.9 eV) and intensities of corresponding $Rh3d_{5/2}$ lines in the spectrum of the resulting copolymer remained practically unchanged (Fig. 3, spectra *5*, *6*), and only a low-intensity line with E_b = 307 eV appeared. Note that we failed to detect a signal from Rh atoms in the XPS spectra of copolymer samples. This fact suggests that the thickness of a polymer shell was greater than 10 nm, that is, the depth of the surface layer accessible to XPS analysis [16]. In other words, it is evident that cluster groups are microencapsulated in a polymer shell. We managed to detect a signal from Rh atoms only after the partial dissolution of the shell.

Cyclohexene hydrogenation in the presence of polymer-immobilized cluster complexes. Cyclohexene hydrogenation is the simplest model reaction of catalytic hydrogenation. To evaluate the catalytic effects of polymer-immobilized cluster complexes and compare them with traditional heterogeneous catalysts, we performed experiments with the synthesized Rh/C sample (Rh content of 1%) with a starting specific activity of 0.1 mol H_2 $(mol\ Rh)^{-1}\ s^{-1}$. As can be seen in Fig. 4, the activity of the test complexes is level with that of the best heterogeneous catalysts. Along with the polymer-immobilized cluster complexes, their low-molecular-weight analogs $Rh_6(CO)_{16}$ (**1**) and $Rh_6(CO)_{15}CH_3CN$ (**2**) were also tested as catalysts in

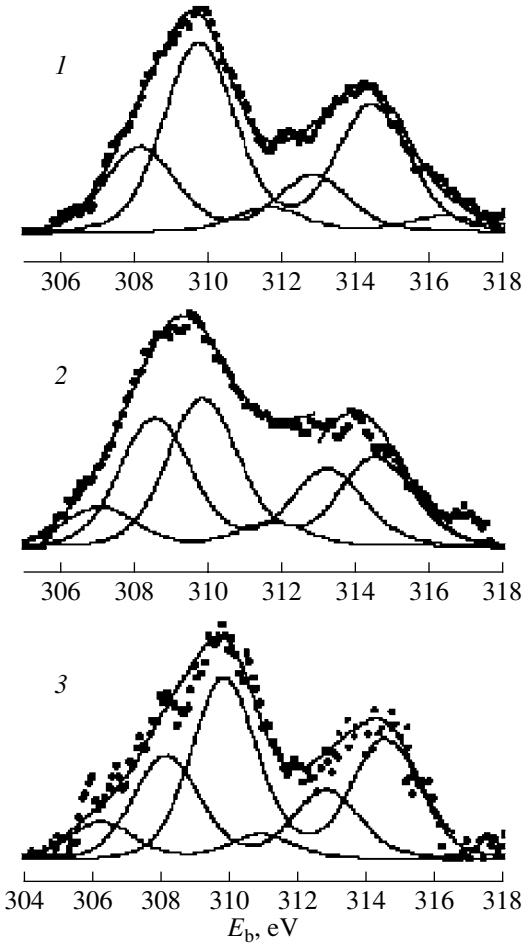

Fig. 3. Rh3*d* XPS spectra of (*1*) $Rh_6(CO)_{14}[\mu,\eta^2\text{-}PPh_2CH_2–CH=CH_2]$, (*2*) $Rh_6(CO)_{14}[\mu,\eta^2\text{-}PPh_2CH_2–CH=CH_2]$ and styrene copolymer, and (*3*) the above sample after the first hydrogenation cycle.

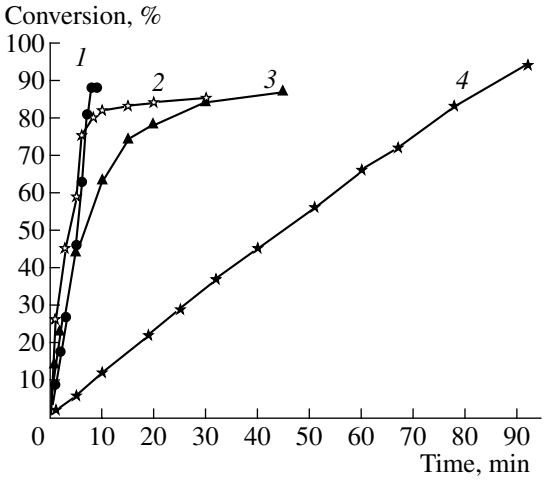

Fig. 4. Hydrogen consumption in the hydrogenation of cyclohexene in the presence of the following catalysts: (*1*) Rh/C, (*2*) copolymer of styrene with $Rh_6(CO)_{14}$(4-VPy)$_2$, (*3*) $Rh_6(CO)_{15}CH_3CN$ immobilized on the styrene and DPPA copolymer (4-SDPPAC), and (*4*) copolymer of styrene with $Rh_6(CO)_{15}$(4-VPy). Catalysis conditions: T = 40°C; P_{H_2} = 1 atm; isopropanol; 3.9×10^{-5} g-at of Rh; 4.5 mmol of the substrate.

this reaction (Fig. 5). In the presence of cluster $Rh_6(CO)_{15}CH_3CN$, the initial specific rate of this reaction at the first loading of the substrate was low (0.006 mol H_2 (g-at Rh)$^{-1}$ s^{-1}); however, it increased to 0.07 mol H_2 (g-at Rh)$^{-1}$ s^{-1} at the second and subsequent loadings. By this is meant that an induction period is required for catalyst activation, in the course of which catalytic centers are formed. In repeated experiments, the rate of hydrogenation increased and the induction period completely disappeared (Fig. 5). The hydrogenation of cyclohexene in the presence of $Rh_6(CO)_{16}$ occurred in another manner: at the first loading of the substrate, the rate of reaction was as high as 0.05 mol H_2 (g-at Rh)$^{-1}$ s^{-1}; at the next loadings, it was 0.07 mol H_2 (g-at Rh)$^{-1}$ s^{-1} and further remained unchanged.

The catalysts based on $Rh_6(CO)_{15}CH_3CN$ immobilized on a copolymer of styrene with DPPA (4-SDPPAC) exhibited high catalytic activity. Although the initial rate of hydrogenation in the presence of the 4-SDPPAC macrocomplex with a rhodium content of 4.16% at the first loading was low (0.02 mol H_2 (g-at Rh)$^{-1}$ s^{-1}), it increased to 0.4 mol H_2 (g-at Rh)$^{-1}$ s^{-1} in the subsequent cycles (Fig. 6). As the catalyst was in operation, the copolymers changed their color from beige to gray. An analogous behavior is characteristic of polymer-immobilized complexes in various reactions [1]; it is related to catalyst working. The heterogenization of the clusters provides an opportunity to separate the catalyst from the reaction medium, to use it repeatedly in new catalytic cycles, and to obtain some experimental evidence for the nature of its intermediates. This would be impossible to perform in homogeneous systems.

The IR spectra of the polymer cluster after hydrogenation exhibited absorption bands characteristic of terminal CO (2066 cm^{-1}), bridging CO (1794 and 1802 cm^{-1}), and P–Ar (1452 cm^{-1}).

In the repeated use of 4-SDPPAC (washed and dried in an inert atmosphere) for cyclohexene hydrogenation, its activity even increased rather than decreased. This was likely due to catalyst development, which was comparatively frequently observed in heterogeneous processes, as noted above. Note that an analogous behavior was found previously with the use of immobilized Os_3 clusters in the catalytic reaction of cyclohexene oxidation [22].

The experimental results allowed us to hypothesize the mechanism of hydrogenation in the presence of the test systems. Thus, the presence of an induction period, the development of a catalyst in the hydrogenation of the next portions of the substrate, a color change in the course of reaction, and the possibility of repeatedly

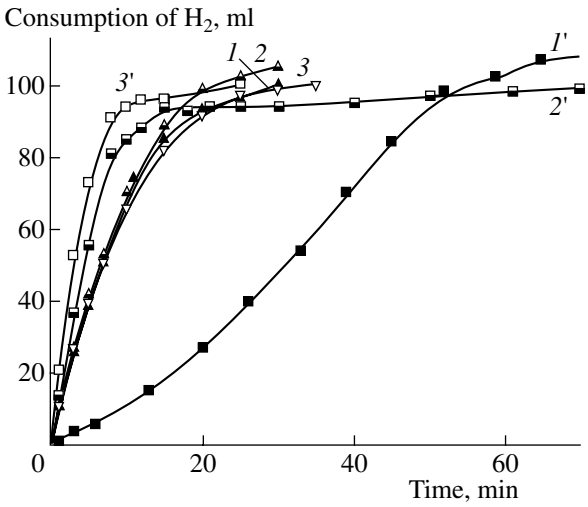

Fig. 5. Curves of hydrogen consumption in the hydrogenation of cyclohexene in the presence of the following monomers: (*1–3*) $Rh_6(CO)_{16}$ (1.2×10^{-4} g-at Rh) and (*1'–3'*) $Rh_6(CO)_{15}CH_3CN$ (1.2×10^{-4} g-at Rh). Curve numbers correspond to cycle numbers. Reaction conditions are specified in Fig. 4.

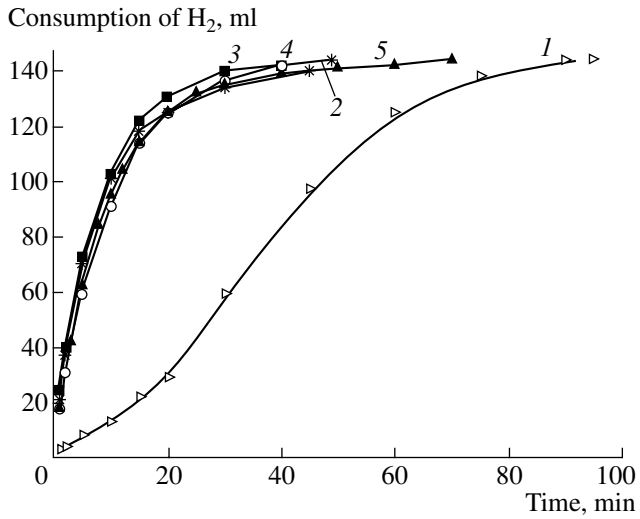

Fig. 6. Curves of hydrogen consumption in the five successive cycles of cyclohexene hydrogenation in the presence of $Rh_6(CO)_{15}CH_3CN$ immobilized on the styrene and DPPA copolymer (4-SDPPAC) (4.16% Rh). Reaction conditions: 3.9×10^{-5} g-at of Rh; $T = 40°C$; $P_{H_2} = 1$ atm; 6.5 mmol of the substrate; solvent, isopropanol. Curve numbers are equal to cycle numbers.

using the catalyst can serve as indirect evidence for cluster fragmentation with the formation of highly active species in low concentrations in the course of hydrogenation. It is likely that the nuclearity of these species is higher (nanosized particles), and they are true catalysts. This hypothesis is also based on the fact that coordination vacancies for hydrogen or a substrate are absent from the Rh_6 carbonyl clusters, including cluster-containing monomers. According to current concepts, active centers in immobilized catalysts are localized at the interfaces of cluster formations, and they are stabilized by their electron systems [1]. It is of importance to note the dynamic character of these systems; their concentration can change in the course of activation of an immobilized complex. Thus, for example, the activity of polymer-immobilized mononuclear rhodium complexes increased with the extents of decarbonylation of rhodium and formation of metal centers including Rh_n^0 [23]. In favorable cases (for example, in the presence of a macromolecular ligand, which prevents the aggregation of cluster particles), a superequilibrium concentration of active states can be produced. This is indirectly evidenced by a comparison between the IR spectra of copolymers before and after hydrogenation: after the reaction, the intensity of bands decreased and they shifted to the region of the vibrations of bridging and terminal carbonyl groups.

XPS data also suggest the formation of these active intermediates. Thus, after the participation of the 4-SDPPAC macrocomplex in the first cycle of cyclohexene hydrogenation, the low-energy line in the Rh3$d_{5/2}$ spectrum shifted to 308.2 eV and a new line appeared at 311 eV (Fig. 2, spectrum *5*). According to Hayden et al. [24], the line with $E_b = 308.2$ eV can correspond to Rh atoms bound to the H(CO) group. The presence of a line at 311 eV after the first cycle of hydrogenation suggests the appearance of Rh atoms with a greater positive charge than that in the parent cluster. The number and positions of the lines in the spectrum remained unchanged after repeatedly performed hydrogenation (Fig. 2, spectrum *6*). Note that hydrogenation resulted in a decrease in the intensity of the main line ($E_b = 309.9$ eV) in the Rh3$d_{5/2}$ spectrum and in an increase in a low-energy spectrum component with $E_b = 308.2$ eV. The relative intensity of the low-energy line in the spectrum of the 4-SDPPAC macrocomplex was 22, 32, or 57% before hydrogenation and after the first or second hydrogenation, respectively. The catalytic activity of the test complex changed symbatically with both the amount of Rh atoms bound to the H(CO) group and the amount of Rh atoms, the charge on which was greater than that in the parent cluster. Note that, in this case, it is likely that the polymer chain bound to the cluster fragment did not undergo considerable changes. This is evidenced by the molecular-weight characteristics of the macrocomplexes before ($M_n = 56000$, $M_w = 140000$, and $M_w/M_n = 2.50$) and after hydrogenation ($M_n = 54000$, $M_w = 127000$, and $M_w/M_n = 2.34$).

Surface characterization of cluster-containing polymers by atomic force microscopy. The images of the surface relief topographies of polymer-immobilized clusters obtained by 3D atomic force microscopy indicate that these clusters were complex multilevel metal–polymer nanocomposites as structured hierarchically

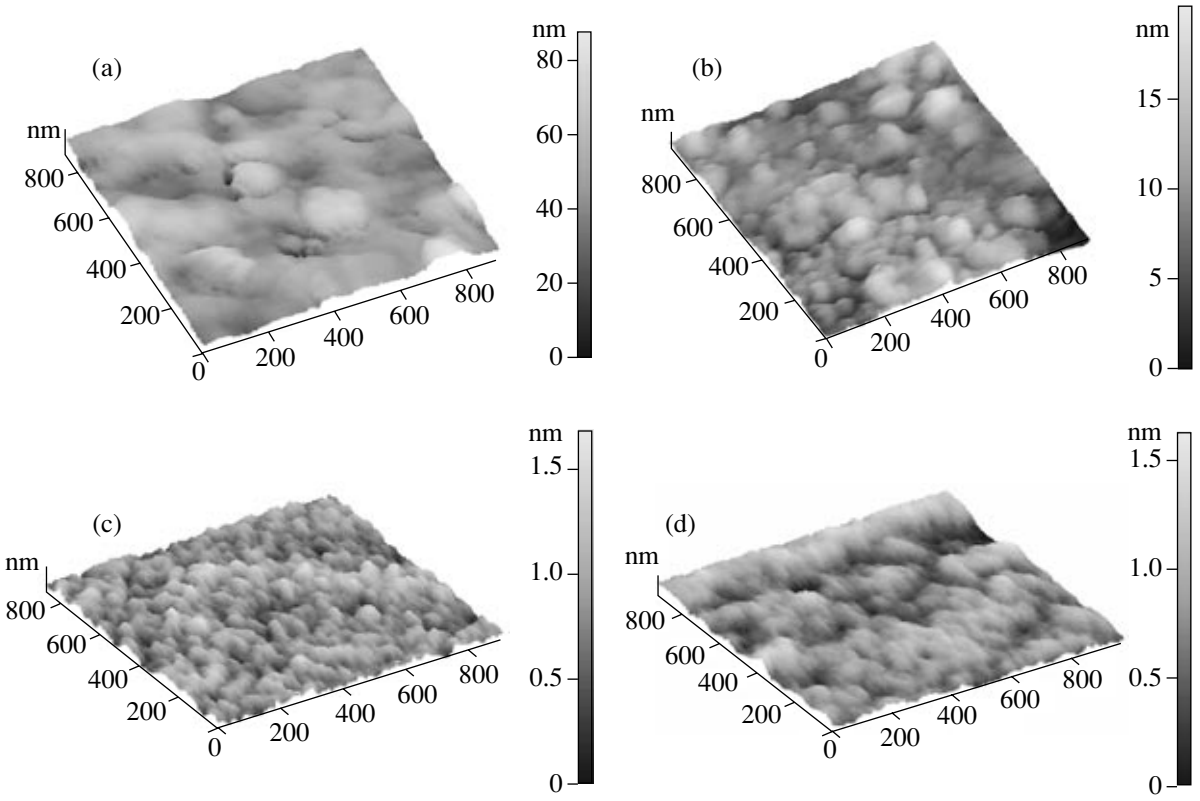

Fig. 7. Morphology of polymer-immobilized cluster particles: (a) 4-SDPPAC macrocomplex, (b) the above sample after the first cycle of hydrogenation, (c) parent copolymer of $Rh_6(CO)_{14}[\mu,\eta^2\text{-}PPh_2CH_2\text{–}CH{=}CH_2]$ with styrene, and (d) the above sample after the first cycle of hydrogenation.

organized particles. The shape of these particles was near-spherical, and the metal–polymer coating was uniformly distributed over the support (Fig. 7). Against the background of 4-SDPPAC macrocomplex particles of size ~20 nm, particle aggregates of size 50–100 nm were predominant. After hydrogenation, the capacity of particles for aggregation weakened, although the main particle size remained unchanged (Fig. 7b). The characteristic particle size of a cluster-containing copolymer of styrene and $Rh_6(CO)_{14}[\mu,\eta^2\text{-}PPh_2CH_2{=}CHCH_2]$ (**3**) was approximately the same as the particle size of the 4-SDPPAC macrocomplex, although the height of individual aggregates was much smaller and they were well separated from each other; because of this, the surface was much more developed (Fig. 7c). After hydrogenation, the capacity of particles for aggregation somewhat increased and a tendency to smoothing was observed. Figure 8 shows the force–distance curves. These curves are plots of cantilever deflection (consequently, the interacting force of the probe with the surface (F_z)) as a function of sample position along the z axis (toward or away from the probe tip). As the sample approached the probe at a certain distance, attracting forces began to act between them. These forces were likely due to the interaction of the probe with moisture adsorbed on the sample surface. The subsequent motion of the sample in the same direction caused sample pressure on the probe, which manifested itself in cantilever deflection (Fig. 8, the direction indicated by arrow *2*). As the sample was removed from the probe, a hysteresis was observed; the cantilever deflection decreased and passed through an equilibrium state (Fig. 8, the direction indicated by arrow *3*). As the sample was further moved, the probe followed the sample under the action of the capillary forces of adsorbed water until the elastic forces of the cantilever became greater than the interacting forces between the probe and the sample. At this point in time, the probe was detached from the sample; the point of cantilever detachment from the sample surface shifted by the value ΔZ, and the cantilever returned to its initial strain-free state (Fig. 8, the direction indicated by arrow *4*). Because capillary forces correlate with surface polarity, the measured forces can serve as a measure of this polarity [25] and, consequently, surface hydrophilicity.

The interacting force F_z between the sample and the probe is determined by the relationship $F_z = k\Delta Z$, where k is the spring constant of the cantilever. The study of the interacting forces between the probe tip and the sample using force–distance curves showed that F_z fell within the range 3–10 nN for 4-SDPPAC particles. The participation of the test macrocomplex in a catalytic

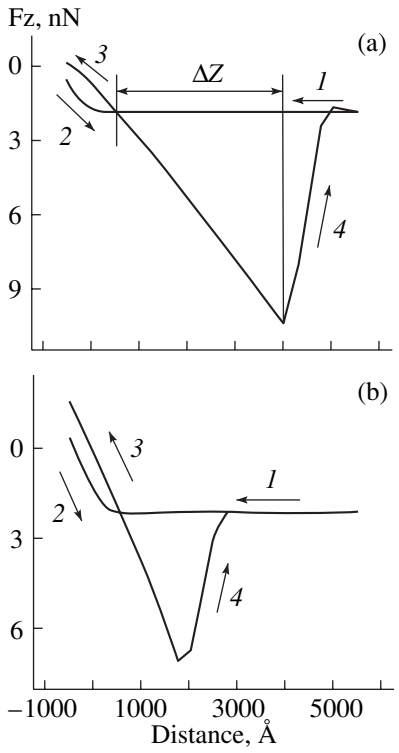

Fig. 8. Force–distance curves for the initial polymer-immobilized clusters: (a) 4-SDPPAC macrocomplex and (b) the copolymer of $Rh_6(CO)_{14}[\mu,\eta^2\text{-}PPh_2CH_2\text{–}CH{=}CH_2]$ with styrene. (*1*) Sample approach to the tip (the tip is in the starting position), (*2*) combined upward motion of the sample with the tip, (*3*) combined backward motion of the sample with the tip, and (*4*) return of the tip to the starting position.

reaction resulted in a decrease in this range and in an increase in F_z. Thus, after the second cycle of hydrogenation, the range of F_z was 8–11 nN. The above data indicate that the surface of 4-SDPPAC macrocomplex particles after hydrogenation became more uniform and hydrophilic. In turn, this suggests an increase in the concentration of polar functional groups in surface layers, which was likely due to the cleavage of Rh–Rh bonds in a cluster.

In the cluster-containing copolymer based on **3**, the range of F_z was 4–6 nN, which is indicative of higher hydrophobicity and uniformity of the surface layers of cluster-containing copolymer particles, as compared with 4-SDPPAC macrocomplex particles. After hydrogenation in the presence of the cluster-containing copolymer based on **3**, the range of F_z remained almost unchanged (4–7 nN); this is indirect evidence for the microencapsulation of the cluster groups of the copolymer in a polymer shell. This hinders transformations in the course of hydrogenation. At the same time, shell parameters allow the substrate and the reaction product to penetrate easily through the shell.

Thus, in this work, we were the first to prepare and characterize polymer-immobilized Rh_6 clusters, which are efficient catalysts for hydrogenation reactions. The heterogenization of metal clusters allowed us to isolate and study some catalytically active intermediates. In the course of catalytic reaction, the cleavage of the Rh–Rh bond and cluster fragmentation occur with the formation of highly active species in low concentrations. It is likely that the nuclearity of these species was greater (nanosized particles), and the hydride forms of these species can be true catalysts. We intend to continue the study of these intermediates, for example, using direct high-resolution transmission electron microscopy.

ACKNOWLEDGMENTS

This study was supported by the Russian Foundation for Basic Research (project nos. 04-03-32634 and 04-03-97233).

REFERENCES

1. Pomogailo, A.D., *Kinet. Katal.*, 2004, vol. 45, no. 1, p. 67 [*Kinet. Catal.* (Engl. Transl.), vol. 45, no. 1, p. 61].
2. Wohrle, D. and Pomogailo, A.D., *Metal Complexes and Metals in Macromolecules*, Weinheim: Wiley-VCH, 2003.
3. Pomogailo, A.D., *Catalysis by Polymer-Immobilized Metal Complexes*, London: Gordon & Breach, 1998.
4. Martinengo, S., Chini, P., and Giordano, G., *J. Organomet. Chem.*, 1971, vol. 27, p. 389.
5. Pomogailo, S.I., Shilov, G.V., Ershova, V.A., Virovets, A.V., Pogrebnyak, V.M., Podberezskaya, N.V., Golovin, A.V., Dzhardimalieva, G.I., and Pomogailo, A.D., *J. Organomet. Chem.*, 2005, vol. 690, p. 4258.
6. *Tekhnologiya katalizatorov* (Catalyst Manufacturing Techniques), Mukhlenov, I.P., Ed., Leningrad: Khimiya, 1974.
7. Povstugar, V.I., Shakov, A.A., Mikhailova, S.S., Voronina, E.V., and Elsukov, E.P., *Zh. Anal. Khim.*, 1998, vol. 53, no. 8, p. 795 [*J. Anal. Chem.* (Engl. Transl.), vol. 53, no. 8, p. 697].
8. Magonov, S.N. and Whangbo, M.-H., *Surface Analysis with STM and AFM*, Weinheim: VCH, 1996.
9. Pomogailo, A.D., *Polimernye immobilizovannye metallokompleksnye katalizatory* (Polymer Immobilized Metal Complex Catalysts), Moscow: Nauka, 1988.
10. Jarrell, M.S., Gates, B.C., and Nicholson, E.D., *J. Am. Chem. Soc.*, 1978, vol. 100, p. 5727.
11. Rafalko, J.J., Lieto, J., Gates, B., and Schrader, G.L., *Chem. Commun.*, 1978, p. 540.
12. Dickson, R.S., *Homogeneous Catalysis with Compounds of Rhodium and Iridium*, Dordrecht: Reidel, 1985.
13. Pomogailo, S.I., Dzhardimalieva, G.I., Ershova, V.A., Aldoshin, S.M., and Pomogailo, A.D., *Macromol. Symp.*, 2002, vol. 186, p. 155.
14. Bravaya, N.M, Pomogailo, A.D., Maksakov, V.A., Kirin, V.P., Grachev, V.P., and Kuzaev, A.I., *Izv. Akad. Nauk, Ser. Khim.*, 1995, no. 6, p. 1102.

15. Fierro, J.L.G., Palacios, J.M., and Tomas, F., *Surf. Interface Anal.*, 1988, vol. 13, p. 25.

16. *Practical Surface Analysis by Auger and X-ray Photoelectron Spectroscopy*, Briggs, D. and Seah, M., Eds., Chichester: Wiley, 1983.

17. Hayden, B.E., King, A., and Newton, M.A., *Surf. Sci.*, 1998, vol. 397, p. 306.

18. Furlani, C., Mattogno, G., Polzonetti, G., Braca, G., and Valentini, G., *Inorg. Chim. Acta*, 1983, vol. 69, p. 199.

19. Carvalho, M., Wieserman, L.F., and Hercules, D.M., *Appl. Spectrosc.*, 1982, vol. 36, p. 290.

20. Andersson, S.L.T. and Scurrell, M.S., *J. Catal.*, 1979, vol. 59, p. 340.

21. Pomogailo, S.I., Chuev, I.I., Dzhardimalieva, G.I., Yarmolenko, A.V., Makhaev, V.D., Aldoshin, S.M., and Pomogailo, A.D., *Izv. Akad. Nauk, Ser. Khim.*, 1999, no. 6, p. 1185.

22. Kholuiskaya, S.N., Pomogailo, A.D., Bravaya, N.M., Pomogailo, S.I., and Maksakov, V.A., *Kinet. Katal.*, 2003, vol. 44, no. 6, p. 831 [*Kinet. Catal.* (Engl. Transl.), vol. 44, no. 6, p. 761].

23. Bhaduri, S. and Khwaja, H., *J. Chem. Soc., Dalton Trans. 1*, 1983, no. 2, p. 419.

24. Hayden, B.E., King, A., and Newton, M.A., *Surf. Sci.*, 1998, vol. 397, p. 306.

25. Anderson, S.L.T. and Scurrell, M.S., *J. Catal.*, 1981, vol. 71, p. 233.